The Investigational Drug VT-1129 is a Highly Potent Inhibitor of *Cryptococcus* species CYP51 but only Weakly Inhibits the Human Enzyme.

Andrew G.S. Warrilow[a], Josie E. Parker[a], Claire L. Price[a], W. David Nes[b], Edward P. Garvey[c], William J. Hoekstra[c], Robert J. Schotzinger[c], Diane E. Kelly[a] and Steven L. Kelly[a*]

Centre for Cytochrome P450 Biodiversity, Institute of Life Science, Swansea University Medical School, Swansea, Wales SA2 8PP, United Kingdom[a]; Center for Chemical Biology, Department of Chemistry and Biochemistry, Texas Tech University, Lubbock, Texas 79409-1061, USA[b]; Viamet Pharmaceuticals, Inc., Durham, NC 27703, USA[c]

Running title: VT-1129 and cryptococcal CYP51s.

Keywords: CYP51, VT-1129, *Cryptococcus*, azole antifungal.

[*]Corresponding author.
Mailing address: Institute of Life Science, Swansea University Medical School, Swansea, Wales SA2 8PP, United Kingdom. Phone: +44 1792 292207 Fax: +44 1792 503430 Email: s.l.kelly@swansea.ac.uk

Cryptococcosis is a life-threatening disease often associated with HIV. Three *Cryptococcus* species CYP51 enzymes were purified and catalyzed the 14α-demethylation of lanosterol, eburicol and obtusifoliol. The investigational agent VT-1129 bound tightly to all three CYP51 proteins (K_d 14 to 25 nM) with similar affinity as fluconazole, voriconazole, itraconazole, clotrimazole and ketoconazole (K_d 4 to 52 nM) whereas VT-1129 bound weakly to human CYP51 (K_d 4.53 μM). VT-1129 was equally as effective as conventional triazole antifungal drugs at inhibiting cryptococcal CYP51 activity (IC_{50} 0.14 to 0.20 μM) while only weakly inhibited human CYP51 activity (IC_{50} ~600 μM). Furthermore, VT-1129 weakly inhibited human CYP2C9, CYP2C19, and CYP3A4 suggesting a low drug-drug interaction potential. Finally, the cellular mode of action for VT-1129 was confirmed to be CYP51 inhibition resulting in the depletion of ergosterol and ergosta-7-enol and the accumulation of eburicol, obtusifolione and lanosterol / obtusifoliol in the cell membranes.

Cryptococcosis is the most common systemic fungal infection in HIV/AIDS immunocompromised patients and is caused by the opportunistic basidiomycete yeast pathogen *Cryptococcus neoformans* (1) leading to infections of the lungs and brain. Meningoencephalitis is the most lethal manifestation of cryptococcosis with a life expectation of less than a month if untreated (2). Pathogenic *Cryptococcus* species cause disease in almost one million people annually with over 620,000 deaths and a third of all HIV/AIDS deaths are attributable to *Cryptococcus* species infection (1). Current treatment options are limited to a handful of drugs, namely initial induction therapy with a combination of amphotericin B and flucytosine followed by a maintenance regime of fluconazole (2). Even after administering the recommended treatment, three-month mortality rates of 10 to 20% are common (3; 4). In addition, adopting such treatment is costly and often impractical (with amphotericin B requiring intravenous administration), especially in developing countries where mortality rates can approach 100% (5; 6).

Three main *C. neoformans* varieties are observed in clinical infections. *C. neoformans var. grubii* (primarily serotype A), ubiquitous in the environment especially in soil, is globally distributed and is responsible for almost all cryptococcal infections in HIV/AIDS patients (6 - 8). *C. neoformans var. neoformans* (primarily serotype D) is less likely to cause severe infection and is more commonly found in Europe (4). *C. neoformans var. gattii* (primarily serotypes B and C), a tree-dwelling basidiomycete yeast primarily located in the tropics and sub-tropics with localized outbreaks in northeast America, is now considered a separate species (*C. gattii*) and is predominantly a primary pathogen infecting healthy (immunocompetent) individuals but will also infect immunocompromised patients if opportunity arises (9). Most

Cryptococcus infections of humans and nearly all infections of HIV/AIDS patients are caused by *C. neoformans var. grubii*, the most prevalent being the H99 strain, although *C. gattii* infection is increasing in prevalence, especially in North America and Africa (9). The taxonomy of *Cryptococcus* species is still evolving with Hagen *et al* (10) proposing that *C. neoformans var. neoformans* and *C. neoformans var. grubii* are separate species and that *C. gattii* consists of five distinct species based on phylogenetic analysis of 11 genetic loci.

Azole resistance, especially towards fluconazole, amongst *Cryptococcus* species in the clinic can be problematic due to prolonged maintenance treatment regimens (11). Increased azole tolerance in *Cryptococcus* species has been attributed to point mutations in CYP51, including G468S and Y145F (12; 13), increased expression levels of CYP51 and the transporter protein AFR1 (14) and the genome plasticity of *Cryptococcus* species post infection (15). Recently an *in silico* three-dimensional model of *C. neoformans* CYP51 has been published (16) with the aim of aiding new drug design. Because many of the marketed azole drugs are limited by a low therapeutic index (17), a drug with a higher therapeutic index might be able to combat resistant pathogens at plasma concentrations still below toxic levels.

In this study we compared the novel tetrazole antifungal VT-1129 (18; 19) (Fig. 1) with clinical azole antifungal drugs in terms of its potency and selectivity of binding to and inhibition of three recombinant cryptococcal CYP51 enzymes compared to human CYP51, and also to human CYPs that are critical xenobiotic-metabolizing enzymes. In addition, the *in vivo* mode of action for VT-1129 was demonstrated through sterol profile analysis.

MATERIALS AND METHODS

Construction of *pCWori$^+$:CneoCYP51*, *pCWori$^+$:CgruCYP51* and *pCWori$^+$:CgatCYP51* expression vectors. The *C. neoformans var. neoformans* CYP51 gene (CneoCYP51 - UniProtKB accession number Q5KQ65), the *C. neoformans var. grubii* CYP51 gene (CgruCYP51 - Q09GQ2) and the *C. gattii* CYP51 gene (CgatCYP51 - E6QZS1) were synthesized by Eurofins MWG Operon (Ebersberg, Germany) incorporating an *Nde*I restriction site at the 5' end and a *Hind*III restriction site at the 3' end of the genes cloned into the pBSIISK$^+$ plasmid. In addition the first eight amino acids were changed to 'MALLLAVF' (20) and a four-histidine extension (CATCACCATCAC) was inserted immediately before the stop codon. The cryptococcal CYP51 genes were excised by *Nde*I / *Hind*III restriction digestion followed by cloning into the pCWori$^+$ expression vector. Gene integrities were confirmed by DNA sequencing.

Heterologous expression and purification of recombinant cryptococcal CYP51 proteins. The *pCWori$^+$:CYP51* constructs were transformed into competent DH5α *E. coli* cells and expressed as previously described (21). Recombinant CYP51 proteins were isolated according to the method of Arase *et al* (22) except that 2% (wt/vol) sodium cholate was used in the sonication buffer and Tween-20 was omitted. The solubilized CYP51 proteins were purified by affinity chromatography using Ni^{2+}-NTA agarose as previously described (23; 21) prior to characterization. The Δ60 truncated human CYP51 was expressed and purified as previously described (24) and was shown to be comparable to the full-length human CYP51 in terms of binding azole antifungal drugs. Protein purities were assessed by SDS polyacrylamide gel electrophoresis.

Cytochrome P450 protein determinations. Reduced carbon monoxide difference spectroscopy was performed (25) with carbon monoxide being passed through the cytochrome P450 solution prior to addition of sodium dithionite to the sample cuvette (light-path 10 mm). An extinction coefficient of 91 mM^{-1} cm^{-1} (26) was used to calculate cytochrome P450 concentrations from the absorbance difference between 447 and 490 nm. Absolute spectra were determined between 700 and 300 nm (light-path 10 mm). All spectral determinations were made using a Hitachi U-3310 UV/VIS spectrophotometer (San Jose, California).

Ligand binding studies. Stock 2.5 mM solutions of lanosterol, eburicol and obtusifoliol were prepared in 40% (wt/vol) (2-hydroxypropyl)-β-cyclodextrin (HPCD) using an ultrasonic bath. Sterol was progressively titrated against 5 μM CYP51 protein in a quartz semi-micro cuvette (light-path 4.5 mm) with equivalent amounts of 40% (wt/vol) HPCD added to the reference cuvette which also contained 5 μM CYP51. The absorbance difference spectrum between 500 and 350 nm was determined after each incremental addition of sterol (up to 75 μM). The sterol saturation curves were constructed from $\Delta A_{390-425}$ derived from the difference spectra. The substrate dissociation constants (K_d) were determined by non-linear regression (Levenberg-Marquardt algorithm) using the Michaelis-Menten equation.

Binding of clotrimazole, fluconazole, voriconazole, itraconazole, ketoconazole and VT-1129 to the cryptococcal CYP51 proteins were performed as previously described (27; 21) using split-cuvettes with a 4.5 mm light-path. Stock 0.1 mg ml^{-1} solutions of the azole antifungal drugs were prepared in dimethylsulfoxide and progressively titrated against 2 μM CYP51 in 0.1 M Tris-HCl (pH 8.1) and 25% (wt/vol)

glycerol. The difference spectra between 500 and 350 nm were determined after each incremental addition of azole and binding saturation curves were constructed from $\Delta A_{peak\text{-}trough}$ against azole concentration. The binding properties of VT-1129 with 5 μM recombinant human CYP51 was also determined (24). The dissociation constants of the enzyme-azole complex (K_d) were determined by non-linear regression (Levenberg-Marquardt algorithm) using a rearrangement of the Morrison equation for 'tight' ligand binding (28; 29). Tight binding occurs where the K_d for a ligand is similar or lower than the concentration of the enzyme present (30).

CYP51 reconstitution assays. Cryptococcal CYP51 reconstitution assays (31; 32) contained 0.5 μM CYP51, 1 μM *Aspergillus fumigatus* cytochrome P450 reductase (AfCPR - UniProtKB accession number Q4WM67), 50 μM lanosterol or 50 μM eburicol or 50 μM obtusifoliol, 50 μM dilaurylphosphatidylcholine, 4% (wt/vol) (2-hydroxypropyl)-β-cyclodextrin (HPCD), 0.4 mg ml^{-1} isocitrate dehydrogenase, 25 mM trisodium isocitrate, 50 mM NaCl, 5 mM $MgCl_2$ and 40 mM MOPS (pH ~7.2). Assay mixtures were incubated at 37°C prior to initiation with 4 mM β-NADPHNa_4 followed by shaking at 37°C for 15 minutes. Human CYP51 reconstitution assays were performed as above except 0.5 μM soluble human CYP51 (24) and 2 μM human cytochrome P450 reductase (P16435) were used and the reaction time reduced to 5 minutes at 37°C. Sterol metabolites were recovered by extraction with ethyl acetate followed by derivatization with *N*,*O*-bis(trimethylsilyl)trifluoroacetamide and tetramethylsilane prior to analysis by gas chromatography mass spectrometry (33).

IC_{50} determinations were performed using 50 µM lanosterol as substrate in which various fluconazole, itraconazole, voriconazole and VT-1129 concentrations in 2.5 µl dimethylsulfoxide were added prior to incubation at 37°C and addition of β-$NADPHNa_4$.

***Cryptococcus* sterol analysis.** *C. neoformans var. neoformans* (strain ATCC MYA-565), *C. neoformans var. grubii* (strain ATCC 208821), and *C. gattii* (strain ATCC MYA-4071) were grown in MOPS buffered RPMI (0.165 M MOPS), pH 7.0, at 37°C and 200 rpm. MOPS buffered RPMI, pH 7.0, in the absence (DMSO control, 1% vol/vol) and presence of fluconazole or VT-1129 was inoculated at a final concentration of 2.5×10^4 cells ml^{-1}. *C. neoformans var. neoformans* was grown in the presence of 0.2 µg ml^{-1} fluconazole or 0.0039 µg ml^{-1} VT-1129; *C. neoformans var. grubii* in the presence of 0.4 µg ml^{-1} fluconazole or 0.0039 µg ml^{-1} VT-1129; *C. gattii* 0.4 µg ml^{-1} fluconazole or 0.0078 µg ml^{-1} VT-1129. Cultures were grown for 2 days at 37°C, 200 rpm and nonsaponifiable lipids were extracted as previously reported (34).

Sterones were MOX-derivatized by the addition of 200 µl of methoxyamine-HCl (2% wt/vol in anhydrous pyridine) incubated for 30 min at 70°C. Samples were mixed with 2 ml of saturated NaCl and the lipids extracted in three sequential 2 ml volumes of ethyl acetate. The combined ethyl acetate fractions were washed with 2 ml volumes of NaCl saturated 0.1 M HCl, saturated NaCl, NaCl saturated 5% wt/vol sodium bicarbonate solution and saturated NaCl. The samples were then dried over anhydrous magnesium sulphate and evaporated using a vacuum centrifuge. Sterols in the dried extracts were derivatized with 0.1 ml BSTFA:TMCS (99:1) and 0.3 ml anhydrous pyridine (2 h at 80°C) prior to analysis by GCMS (33). Individual sterols and sterones

were identified by reference to relative retention times, mass ions and fragmentation patterns. Sterol composition was calculated using peak areas.

Inhibition of human liver CYP enzymes. *In vitro* studies determined the IC_{50} of the test compounds for CYP2C9, CYP2C19, and CYP3A4 (with either midazolam or testosterone as substrates) in intact human liver microsomes. A separate series of incubation mixtures was prepared with each test compound at final concentration in reaction ranging from 0.0128 to 200 μM. Each incubation mixture contained pooled human liver microsomes at an assay concentration of 1 mg ml^{-1} microsomal protein (Life Technologies, Grand Island, NY) and metabolic substrates of isozymes for CYP2C9, CYP2C19, and CYP3A4 (diclofenac, omeprazole, and midazolam or testosterone, respectively) at their experimentally determined K_m concentrations. Active control wells contained microsomes, substrate(s), and the test-compound diluent (i.e. DMSO:acetonitrile:phosphate buffer, 5:5:190) substituted for test compound solutions. The reaction was initiated by addition of an enzyme cofactor source (NADPH regenerating solution; BD Biosciences, San Jose, CA) and the mixtures were incubated at 37°C. After ten minutes, incubation mixtures were quenched with acetonitrile, mixed, and centrifuged. The supernatant was analyzed by HPLC-MS/MS for the hydroxy metabolite of the substrates. Each product peak area was normalized to be represented as a percentage of the enzyme control average. The IC_{50} value for each test compound was determined by fitting a 4-parameter logistical fit to the dose response data and graphically determining the inhibitor concentration at 50% of the maximal enzymatic response.

198 **Data analysis.** All ligand binding experiments were performed in triplicate and
199 curve-fitting of data performed using the computer program ProFit 6.1.12 (QuantumSoft,
200 Zurich, Switzerland). GC/MS data were analyzed using Thermo Xcalibur 2.2 software.
201 **Chemicals.** VT-1129 was provided by Viamet Pharmaceuticals, Inc. (Durham,
202 USA). All other chemicals were obtained from Sigma Chemical Company (Poole, UK).
203 Growth media, sodium ampicillin, IPTG and 5-aminolevulenic acid were obtained from
204 Foremedium Ltd (Hunstanton, UK). Ni^{2+}-NTA agarose affinity chromatography matrix
205 was obtained from Qiagen (Crawley, UK).
206
207

RESULTS

Expression and purification of cryptococcal CYP51 proteins. Following heterologous expression in *E. coli*, CneoCYP51, CgruCYP51 and CgatCYP51 were extracted by sonication with 2% (wt/vol) sodium cholate (22), which yielded 240 (±90), 160 (±50) and 290 (±80) nmoles per liter culture as determined by carbon monoxide difference spectroscopy (25). Purification by chromatography on Ni^{2+}-NTA agarose resulted in 70%, 54% and 45% recoveries of native CneoCYP51, CgruCYP51 and CgatCYP51 proteins, respectively. SDS polyacrylamide gel electrophoresis confirmed the purity of Ni^{2+}-NTA agarose eluted cryptococcal CYP51 proteins to be greater than 90% when assessed by staining intensity, with apparent molecular weights of 55,000 to 58,000 compared to the predicted values of 62,708 (Cneo), 62,310 (Cgru), and 62,689 (Cgat) including N-terminal modifications and 4 His C-terminal extensions.

Spectral properties of cryptococcal CYP51 proteins. The absolute spectra of the resting oxidized forms of all three CYP51 proteins (Fig. 2A) were typical for a low-spin ferric cytochrome P450 enzyme (23; 35) with α, β, Soret (γ) and δ spectral bands at 566, 536, 418 and 360 nm, respectively. Reduced carbon monoxide difference spectra (Fig. 2B) gave the red-shifted heme Soret peak at 447 nm, characteristic of P450 enzymes, indicating that all three CYP51 proteins were expressed in the native form.

Sterol binding properties of cryptococcal CYP51 proteins. Progressive titration with lanosterol, eburicol and obtusifoliol gave characteristic type I difference spectra for all three CYP51 proteins with a peak at 390 nm and a trough at 425 nm (Fig. 3). Type I binding spectra occur when the substrate or another molecule displaces the water molecule coordinated as the sixth ligand to the low-spin hexa-coordinated heme prosthetic group causing the heme to adopt the high-spin penta-coordinated

conformation (35). The cryptococcal CYP51 proteins had similar affinities for the three sterols (Table 1) with K_d values of 16 to 18 μM for lanosterol, 12 to 16 μM for eburicol and 12 to 21 μM for obtusifoliol. This suggested that all three 14α-methylated sterols were potential substrates for the cryptococcal CYP51 proteins.

The sterol binding affinities of the three cryptococcal CYP51 proteins (K_d values 12 to 21 μM) were similar to those reported for other CYP51 proteins. For example, K_d values for lanosterol and eburicol were 11-16 and 25-28 μM with *Candida albicans* CYP51 (21), 11 and 13 μM with *Mycosphaerella graminicola* CYP51 (36) and 0.5 to 18 μM for lanosterol with human CYP51 (37; 38; 24). However, the sterol K_d values obtained were 10- to 20-fold higher than those obtained for lanosterol with *Mycobacterium tuberculosis* CYP51 (1 μM) (23) and for lanosterol and eburicol with *Trypanosoma cruzei* CYP51 (1.9 and 1.2 μM) (32).

CYP51 reconstitution assays. CYP51 assays using 50 μM sterol gave turnover numbers of 1.2 to 1.9 min^{-1} for lanosterol, 3.7 to 7.6 min^{-1} for eburicol and 3.5 to 4.5 min^{-1} for obtusifoliol (Table 1), confirming that all three cryptococcal CYP51 proteins readily catalyzed the 14α-demethylation of these three sterols. Both CneoCYP51 and CgruCYP51 displayed a substrate preference for eburicol over obtusifoliol and lanosterol whilst CgatCYP51 displayed a substrate preference for obtusifoliol over eburicol and lanosterol. The ability of CgatCYP51, in particular, to readily demethylate obtusifoliol indicates a preference for C-24 methylated sterol substrate.

Azole binding properties of CYP51 proteins. All five medical azole antifungal agents and the investigation agent VT-1129 bound tightly to all three cryptococcal CYP51 proteins producing type II binding spectra. The binding spectra and saturation

curves obtained for fluconazole and itraconazole (Fig. 4) and VT-1129 (Fig. 5) are shown with a peak at ~429 nm and a trough at ~412 nm. Type II binding spectra are caused by the triazole ring N-4 nitrogen (fluconazole, itraconazole and voriconazole) or the imadazole ring N-3 nitrogen (clotrimazole, ketoconazole) coordinating as the sixth ligand with the heme iron (39) to form the low-spin CYP51-azole complex resulting in a 'red-shift' of the heme Soret peak. The interaction of VT-1129 with the heme ferric ion is through a terminal (N-3 or N-4) tetrazole nitrogen atom. CneoCYP51 bound the azole antifungal agents the strongest with apparent K_d values of 4 to 11 nM (Table 1), followed by CgatCYP51 with apparent K_d values of 5 to 24 nM and CgruCYP51 bound the azole antifungal agents the weakest with apparent K_d values of 14 to 52 nM. None of the cryptococcal CYP51 enzymes appeared to be inherently resistant to azole antifungal agents as the range of K_d values observed (4 to 52 nM) were similar to those observed with *C. albicans* CYP51 (10 to 56 nM) (24), unlike *Aspegillus fumigatus* CYP51A which appeared to be inherently resistant to fluconazole with an apparent K_d value of 11.9 μM (40). The binding affinity of VT-1129 to all three cryptococcal CYP51 proteins was strong (K_d 11 to 25 nM) and similar to the other five clinical azole antifungal agents examined, suggesting VT-1129 would be effective as a therapeutic agent against *Cryptococcus* species infections. The similar azole binding properties of the three cryptococcal CYP51 proteins agrees with their close sequence homology with CneoCYP51 sharing 98% and 96% sequence identity with CgruCYP51 and CgatCYP51.

In contrast, VT-1129 bound relatively weakly to human CYP51 (Fig. 5) with an apparent K_d of 4.53 μM (Table 1). The interaction of VT-1129 with human CYP51 was atypical as it gave rise to a red-shifted type I difference spectrum (peak at 410 nm and trough at 426 nm) rather than the expected type II difference spectrum normally

observed for the interaction of azole antifungal agents with CYP51 proteins. This suggests that the mode of interaction of VT-1129 with the human CYP51 was different to that observed with the three cryptococcal CYP51 proteins. VT-1129 still perturbs the heme environment of human CYP51 as a difference spectrum was observed, though not through the azole nitrogen directly coordinating with the heme ferric ion. This altered interaction of VT-1129 with human CYP51 resulted in very weak inhibition of CYP51 activity in the CYP51 reconstitution assay (see below). The K_d values obtained for VT-1129 with the cryptococcal CYP51 enzymes were 180- to 410-fold lower than that obtained with the human homolog, confirming the high selectivity of VT-1129 for the fungal target enzyme. This compared favorably with fluconazole and voriconazole, which gave K_d values that were 370- to 1300-fold and 120- to 570-fold lower for cryptococcal CYP51 enzymes than human CYP51. VT-1129 exhibited far greater selectivity towards cryptococcal CYP51 enzymes over the human homolog than clotrimazole, ketoconazole of itraconazole, which exhibited K_d values that were only 1.3- to 15-fold lower for the fungal CYP51 than human CYP51.

Azole IC_{50} determinations. IC_{50} determinations (Fig. 6) confirmed that all three cryptococcal CYP51 proteins bound fluconazole, itraconazole voriconazole and VT-1129 tightly giving rise to strong inhibition of the CYP51 demethylation of lanosterol. IC_{50} values of 0.14 to 0.20 μM (Table 1) were obtained which were close to half the CYP51 concentration present in the assay system. VT-1129 proved equally as effective at inhibiting cryptococcal CYP51 activity as the three other azole antifungal drugs, suggesting VT-1129 would be effective at combating *Cryptococcus* infections. In contrast, VT-1129 only weakly inhibited human CYP51 activity (IC_{50} ~600 μM) (Fig. 7) in agreement with the weak perturbation of the heme environment of human CYP51

observed with VT-1129 (Fig. 5), whereas clotrimazole severely inhibited human CYP51 activity (IC_{50} 1.9 μM). The IC_{50} values observed for VT-1129 with the cryptococcal CYP51 enzymes were 3300- to 4000-fold lower than that obtained with the human homolog (Table 1), again confirming high selectivity for the fungal target enzyme. This was comparable to fluconazole where the IC_{50} value obtained with the fungal CYP51 enzymes were 6500- to 9000- fold lower than with human CYP51 and significantly better than the observed selectivity with voriconazole and itraconazole (Table 1). The IC_{50} values for VT-1129 were more potent than the K_d values for binding to cryptococcal CYP51 enzymes, suggesting that the Morrison equation calculated K_d values were an overestimate in part due to the relatively high CYP51 protein concentrations required for *in vitro* binding studies.

***Cryptococcus* sterol content.** The treatment of *Cryptococcus* spp. with 0.2 to 0.4 μg ml^{-1} fluconazole and 0.0039 to 0.0078 μg ml^{-1} VT-1129 resulted in the accumulation of eburicol (Table 2), obtusifolione and lanosterol / obtusifoliol. Accumulation of CYP51 substrates is indicative of direct CYP51 inhibition in treated cells. Both azole treatments resulted in the depletion of the post-CYP51 sterol metabolites ergosta-7,22-dienol and ergosta-7-enol and the partial depletion of ergosterol levels (Table 2) showing CYP51 inhibition. In these cellular experiments, VT-1129 was significantly more potent than fluconazole, as VT-1129 had caused greater inhibition of cryptococcal CYP51 activity at fifty-fold lower concentrations than fluconazole (relative to DMSO control, VT-1129 caused greater reductions in ergosterol levels compared to fluconazole at 50-fold higher concentrations and in all cases accumulation of 14-methylated product showing CYP51 was inhibited in cells; Table 2).

326 **Inhibition of human liver drug metabolizing CYPs.** Inhibition of three critical
327 xenobiotic-metabolizing CYPs by the four approved azole drugs and VT-1129 are shown
328 in Table 3. Where available, the literature IC_{50} values for the marketed agents (41 - 43)
329 agree well with those measured in this study. The imidazole-containing clotrimazole was
330 the most potent CYP inhibitor, inhibiting all activities with sub- or low-micromolar
331 potency. The three triazole-containing agents had variable inhibitory potencies, with
332 itraconazole potently inhibiting CYP3A4 with either substrate (0.08 and 0.13 μM),
333 voriconazole inhibiting all activities with a relatively tight range of potencies (4 to 13 μM),
334 and fluconazole showing a slightly broader range (6 to 34 μM). In contrast, VT-1129
335 weakly inhibited each of these activities (79 to 178 μM).
336
337

DISCUSSION

Sionov *et al* (14) demonstrated that *C. neoformans* strains are heteroresistant to fluconazole with each strain yielding a sub-population that can survive fluconazole concentrations well above the MIC values through disomy of chromosome 1 which duplicates the CYP51 and AFR1 transporter genes. Disomy of chromosome 1 coupled with reported G468S and Y145F CYP51 mutations (12; 13), increased CYP51 and AFR1 expression levels (14) and the genome plasticity post infection (15) may explain the divergent range of MIC values reported for fluconazole with *Cryptococcus* spp. of 0.5 to 64 μg ml^{-1} (44 - 47). MIC values reported for voriconazole (0.008 to 0.5 μg ml^{-1}), itraconazole (0.015 to 0.5 μg ml^{-1}) and posaconazole (0.008 to 0.5 μg ml^{-1}) were lower and less variable than for fluconazole (44 - 47), indicating therapeutic efficacy of these triazole antifungals should fluconazole-tolerance become problematic. However, as previously observed with *Candida* spp. and *Aspergillus* spp., it can be anticipated that azole tolerance will emerge against current triazole therapeutics in *Cryptococcus* spp.

New antifungal drug candidates for the treatment of systemic *Cryptococcus* infection which target CYP51 should ideally have high potency against the intended cryptococcal CYP51 target enzymes and minimal interaction with human CYP51 and other critical CYP enzymes such as those that metabolize xenobiotics. VT-1129 meets both these criteria by binding tightly to cryptococcal CYP51 enzymes (K_d values 11 to 25 nM) with similarly high affinity as other pharmaceutical azole antifungal agents (K_d values 4 to 52 nM) whilst binding weakly to the host human CYP51 *in vitro* (K_d 4.53 μM). Binding studies (Fig. 4 and 5) provide useful preliminary information on a 'cyclized nitrogen-containing' antifungal drug-candidate's likely effectiveness at inhibiting CYP51 activity. However, only IC_{50} determinations using a CYP51 reconstitution assay system

can determine the functional activity of each compound as a CYP51 inhibitor. IC_{50} determinations confirmed that VT-1129 was a strong inhibitor of cryptococcal CYP51 activity consistent with tight-binding inhibition but only weakly inhibited human CYP51 (13% inhibition at 150 µM VT-1129). VT-1129 selectivity for the cryptococcal CYP51 protein over the human homolog was ~3300-fold in terms of inhibiting CYP51 catalysis and VT-1129 was equally effective as conventional triazole antifungal drugs at inhibiting cryptococcal CYP51 activity. VT-1129's selectivity for inhibiting cryptococcal CYP51 was similarly high when compared to key human xenobiotic-metabolizing CYPs, suggesting a low potential for clinical drug-drug interactions.

Sterol profile analysis confirmed that VT-1129 inhibited cryptococcal CYP51 activity in whole cells, resulting in the depletion of ergosterol and ergosta-7-enol from the cell membranes and the accumulation of 14-methylated compounds eburicol and lanosterol / obtusifoliol and obtusifolione. In a separate study measuring a large number of *Cryptococcus* spp. isolates and using 50% inhibition as the endpoint, the MIC_{90} for VT-1129 was 0.060 µg ml^{-1} against 180 isolates of *C. neoformans* and 0.25 µg ml^{-1} against 321 isolates of *C. gattii* (19) confirming that VT-1129 is a potent inhibitor of *Cryptococcus* spp. growth. In both studies, VT-1129 was a more potent inhibitor of *Cryptococcus* spp. CYP51 than fluconazole. In addition, VT-1129 retains all or most of its antifungal potency against 50 Ugandan clinical isolates of *C. neoformans* with elevated fluconazole MIC values (48). This potency coupled with its excellent selectivity versus human CYP enzymes shown here supports VT-1129 as a good candidate for the treatment of systemic *Cryptococcus* infections. Given the unmet need for more potent drugs for this disease especially in sub-Saharan Africa further assessment towards

clinical trials are warranted, with VT-1129 Phase 1 studies now underway in healthy volunteers.

ACKNOWLEDGMENT

We are grateful to the Engineering and Physical Sciences Research Council National Mass Spectrometry Service Centre at Swansea University and Mr. Marcus Hull for assistance in GC/MS analyses.

This work was in part supported by the European Regional Development Fund / Welsh Government funded BEACON research program (Swansea University), the National Science Foundation of the United States grant NSF-MCB-09020212 awarded to W. David Nes (Texas Tech University) and by Viamet Pharmaceuticals Inc (Durham, NC 27703, USA).

REFERENCES

1. **Park BJ, Wannemuehler KA, Marston BJ, Govender N, Pappas PG, Chiller TM.** 2009. Estimation of the current global burden of cryptococcal meningitis among persons living with HIV/AIDS. Aids. **23:**525-530.
2. **Bicanic T, Harrison TS.** 2004. Cryptococcal meningitis. Br. Med. Bull. **72:**99-118.
3. **Lortholary O, Poizat G, Zeller V, Neuville S, Boibieux A, Alvarez M, Dellamonica P, Botterel F, Dromer F, Chene G, and the French Cryptococcosis study group.** 2006. Long-term outcome of AIDS-associated cryptococcosis in the era of combination antiretroviral therapy. Aids. **20:**2183-2191.
4. **Dromer F, Mathoulin-Pelissier S, Launay O, Lortholary O.** 2007. Determinants of disease presentation and outcome during cryptococcosis: the Crypto A/D study. PLoS Med. **4:**e21.
5. **Mwaba P, Mwansa J, Chintu C, Pobee J, Scarborough M, Portsmouth S, Zumla A.** 2001. Clinical presentation, natural history, and cumulative death rates of 230 adults with primary cryptococcal meningitis in Zambian AIDS patients treated under local conditions. Postgrad. Med. J. **77:**769-773.
6. **French N, Gray K, Watera C, Nakiyingi J, Lugada E, Moore M, Lalloo D, Whitworth JAG, Gilks CF.** 2002. Cryptococcal infection in a cohort of HIV-1-infected Ugandan aldults. Aids. **16:**1031-1038.
7. **Canteros CE, Brundy M, Rodero L, Perrotta D, Davel G.** 2002. Distribution of *Cryptococcus neoformans* serotypes associated with human infections in Argentina. Rev. Argent. Microbiol. **34:**213-218.

8. **Banerjee U, Datta K, Casadevall A.** 2004. Serotype distribution of *Cryptococcus neoformans* in patients in a tertiary care center in India. Med. Mycol. **242:**181-186.

9. **Byrnes EJ, Bartlett KH, Perfect JR, Heitman J.** 2011. *Cryptococcus gattii*: an emerging fungal pathogen infecting humans and animals. Microbes Infect. **13:**895-907.

10. **Hagen F, Khayhan K, Theelen B, Kolecka A, Polacheck I, Sionev E, Falk R, Parnmen S, Lumbsch HT, Boekhout T.** 2015. Recognition of seven species in the *Cryptococcus gattii* / *Cryptococcus neoformans* species complex. Fungal Genet. Biol. **78:**16-48.

11. **Perfect JR, Cox GM.** Drug resistance in *Cryptococcus neoformans*. 1999. Drug Resist. Update. **2:**259-269.

12. **Rodero L, Mellado E, Rodriguez AC, Salve A, Guelfand L, Cahn P, Cuenca-Estrella M, Davel G, Rodriguez-Tudela JL.** 2003. G484S amino acid substitution in lanosterol 14-α.demethylase (ERG11) gene in *Cryptococcus neoformans*. Biochem. Biophys. Res. Comm. **324:**719-728.

13. **Sionov E, Chang YC, Garraffo HM, Dolan MA, Ghannoum MA, Kwon-Chung KJ.** 2012. Identification of a *Cryptococcus neoformans* cytochrome P450 lanosterol 14α-demethylase (Erg11) residue critical for differential susceptibility between fluconazole/voriconazole and itraconazole/posaconazole. Antimicrob. Agents Chemother. **56:**1162-1169.

14. **Sionov E, Lee H, Chang YC, Kwon-Chung KJ.** 2010. *Cryptococcus neoformans* overcomes stress of azole drugs by formation of disomy in specific multiple chromosomes. PLoS Pathogens. **6:**e1000848.

15. **Hu G, Wang J, Choi J, Jung WH, Liu I, Litvintseva AP, Bicanic T, Aurora R, Mitchell TG, Perfect JR, Kronstad JW.** 2011. Variation in chromosome copy number influences the virulence of *Cryptococcus neoformans* and occurs in isolates from AIDS patients. BMC Genomics. **12:**526.

16. **Sheng C, Miao Z, Ji H, Yao J, Wang W, Che X, Dong G, Lu J, Guo W, Zhang W.** 2009. Three-dimensional model of lanosterol 14α-demethylase from *Cryptococcus neoformans*: active-site characterization and insights into azole binding. Antimicrob. Agents Chemother. **53:**3487-3495.

17. **Suzuki Y, Tokimatsu I, Sato Y, Kawasaki K, Sato Y, Goto T, Hashinaga K, Itoh H, Hiramatsu K, Kadota J.** 2013. Association of sustained high plasma trough concentration of voriconazole with the incidence of hepatotoxicity. Clin. Clim. Acta. **424:**119-122.

18. **Hoekstra WJ, Garvey EP, Moore WR, Rafferty SW, Yates CM, Schotzinger RJ.** 2014. Design and optimization of highly-selective fungal CYP51 inhibitors. Bioorg. Med. Chem. Lett. **24:**3455-3458.

19. **Lockhart SR, Fothergill AW, Iqbal N, Bolden CB, Grossman NT, Garvey EP, Brand SR, Hoekstra WJ, Schotzinger RJ, Ottinger E, Patterson TF, Wiederhold NP.** 2016. The investigational fungal Cyp51 inhibitor VT-1129 demonstrates potent in vitro activity against *Cryptococcus neoformans* and *Cryptococcus gattii*. Antimicrob. Agents Chemother. In press AAC.02770-15.

20. **Barnes HJ, Arlotto MP, Waterman MR.** 1991. Expression and enzymatic activity of recombinant cytochrome P450 17α-hydroxylase in *Escherichia coli*. Proc. Natl. Acad. Sci. USA. **88:**5597-5601.

21. **Warrilow AGS, Martel CM, Parker JE, Melo N, Lamb DC, Nes D, Kelly DE, Kelly SL.** 2010. Azole binding properties of *Candida albicans* sterol 14-α demethylase (CaCYP51). Antimicrob. Agents Chemother. **54:**4235-4245.

22. **Arase M, Waterman MR, Kagawa N.** 2006. Purification and characterization of bovine steroid 21-hydroxylase (P450c21) efficiently expressed in *Escherichia coli*. Biochem. Biophys. Res. Com. **344:**400-405.

23. **Bellamine A, Mangla AT, Nes WD, Waterman MR. 1999.** Characterisation and catalytic properties of the sterol 14α-demethylase from *Mycobacterium tuberculosis*. Proc. Natl. Acad. Sci. USA. **96:**8937-8942.

24. **Warrilow AGS, Parker JE, Kelly DE, Kelly SL.** 2013. Azole affinity of sterol 14α-demethylase (CYP51) enzymes from *Candida albicans* and *Homo sapiens*. Antimicrob. Agents Chemother. **57:**1352-1360.

25. **Estabrook RW, Peterson JA, Baron J, Hildebrandt AG.** 1972. The spectrophotometric measurement of turbid suspensions of cytochromes associated with drug metabolism, p 303-350. In: Chignell CF (ed), Methods in Pharmacology, vol 2, Appleton-Century-Crofts, New York, NY.

26. **Omura T, Sato R.** 1964. The carbon monoxide-binding pigment of liver microsomes. J. Biol. Chem. **239:**2379-2385.

27. **Lamb DC, Kelly DE, Waterman MR, Stromstedt M, Rozman D, Kelly SL.** 1999. Characteristics of the heterologously expressed human lanosterol 14α-demethylase (other names: P45014DM, CYP51, P45051) and inhibition of the purified human and *Candida albicans* CYP51 with azole antifungal agents. Yeast **15:**755-763.

494 28. **Lutz JD, Dixit V, Yeung CK, Dickmann LJ, Zelter A, Thatcher JA, Nelson WL,**
495 **Isoherranen N.** 2009. Expression and functional characterization of cytochrome
496 P450 26A1, a retinoic acid hydroxylase. Biochem. Pharmacol. **77:**258-268.
497 29. **Morrison JF.** 1969. Kinetics of the reversible inhibition of enzyme-catalysed
498 reactions by tight-binding inhibitors. Biochim. Biophys. Acta – Enzymol. **185:**269-
499 286.
500 30. **Copeland RA.** 2005. Evaluation of enzyme inhibitors in drug discovery: a guide
501 for medicinal chemists and pharmacologists, p 178-213, Wiley-Interscience, New
502 York, NY.
503 31. **Lepesheva GI, Ott RD, Hargrove TY, Kleshchenko YY, Schuster I, Nes WD,**
504 **Hill GC, Villalta F, Waterman MR.** 2007. Sterol 14α-demethylase as a potential
505 target for antitrypanosomal therapy: enzyme inhibition and parasite cell growth.
506 Chem. Biol. **14:**1283–1293.
507 32. **Lepesheva GI, Zaitseva NG, Nes WD, Zhou W, Arase M, Liu J, Hill GC,**
508 **Waterman MR.** 2006. CYP51 from *Trypanosoma cruzi*: a phyla-specific residue
509 in the B' helix defines substrate preferences of sterol 14α-demethylase. J. Biol.
510 Chem. **281:**3577–3585.
511 33. **Parker JE, Warrilow AGS, Cools HJ, Fraaije BA, Lucas JA, Rigdova K,**
512 **Griffiths WJ, Kelly DE, Kelly SL.** 2011. Prothioconazole and prothioconazole-
513 desthio activity against *Candida albicans* sterol 14α-demethylase (CaCYP51).
514 Appl. Environ. Microbiol. **79:**1639-1645.
515 34. **Kelly SL, Lamb DC, Corran AJ, Baldwin BC, Kelly DE.** 1995. Mode of action
516 and resistance to azole antifungals associated with the formation of 14α-

methylergosta-8,24(28)-dien-3β,6α-diol. Biochem. Biophys. Res. Comm. **207:**910-915.

35. **Jefcoate CR.** 1978. Measurement of substrate and inhibitor binding to microsomal cytochrome P-450 by optical-difference spectroscopy. Methods Enzymol. **52:**258-279.

36. **Parker JE, Warrilow AGS, Cools HJ, Martel CM, Nes WD, Fraaije BA, Lucas JA, Kelly DE, Kelly SL.** 2011. Mechanism of binding of prothioconazole to *Mycosphaerella graminicola* CYP51 differs from that of other azole antifungals. Appl. Environ. Microbiol. **77:**1460-1465.

37. **Lepesheva GI, Nes WD, Zhou W, Hill GC, Waterman MR.** 2004. CYP51 from *Trypanosoma brucei* is obtusifoliol-specific. Biochemistry **43:**10789–10799.

38. **Strushkevich N, Usanov SA, Park HW.** 2010. Structural basis of human CYP51 inhibition by antifungal azoles. J. Mol. Biol. **397:**1067-1078.

39. **Jefcoate CR, Gaylor JL, Calabrese RL.** 1969. Ligand interactions with cytochrome P450. I. Binding of primary amines. Biochemistry **8:**3455-3463.

40. **Warrilow AGS, Melo N, Martel CM, Parker JE, Nes D, Kelly DE, Kelly SL.** 2010. Expression, purification, and characterization of *Aspergillus fumigatus* sterol 14-α demethylase (CYP51) isoenzymes A and B. Antimicrob. Agents Chemother. **54:**4225-4234.

41. **Niwa T, Shiraga T, Takagi A.** 2005. Effect of antifungal drugs on cytochrome P450 (CYP) 2C9, CYP2C19, and CYP3A4 activities in human liver microsomes. Biol. Pharm. Bull. **28:**1805-1808.

42. **Zhang S, Pillai VC, Mada SR, Strom S, Venkataramanan R.** 2012. Effect of voriconazole and other azole antifungal agents on CYP3A activity and metabolism of tacrolimus in human liver microsomes. Xenobiotica **42:**409-416.

43. **Zhang W, Ramamoorthy Y, Kilicarslan T, Nolte H, Tyndale RF, Sellers EM.** 2002. Inhibition of cytochromes P450 by antifungal imidazole derivatives. Drug Met. Disp. **30:**314-318.

44. **Trilles L, Meyer W, Wanke B, Guarro J, Lazera M.** 2012. Correlation of antifungal susceptibility and molecular type within the *Cryptococcus neoformans* / *C. gattii* species complex. Med. Mycol. **50:**328-332.

45. **Pfaller MA, Castanheira M, Messer SA, Moet GJ, Jones RN.** 2011. Echinocandin and triazole antifungal susceptibility profiles for *Candida* spp., *Cryptococcus neoformans*, and *Aspergillus fumigatus*: application of new CLSI clinical breakpoints and epidemiologic cutoff values to characterize resistance in the SENTRY antimicrobial surveillance program (2009). Diag. Microbiol. Infect. Dis. **69:**45-50.

46. **Bertout S, Drakulovski P, Kouanfack C, Krasteva D, Ngouana T, Dunyach-Remy C, Dongsta J, Aghokeng A, Delaporte E, Koulla-Shiro S, Reynes J, Mallie M.** 2012. Genotyping and antifungal susceptibility testing of *Cryptococcus neoformans* isolates from Cameroonian HIV-positive adult patients. Clin. Microbiol. Infect. **19:**763-769.

47. **Lockhart SR, Iqbal N, Bolden CB, DeBess EE, Marsden-Haug N, Worhle R, Thakur R, Harris JR.** 2012. Epidemiologic cutoff values for triazole drugs in *Cryptococcus gattii*: correlation of molecular type and in vitro susceptibility. Diag. Microbiol. Infect. Dis. **73:**144-148.

48. **Vedula P, Smith K, Boulware DR, Meya DB, Garvey EP, Hoekstra WJ, Schotzinger RJ, Nielsen K.** 2015. Activity of VT-1129 against *Cryptococcus neoformans* clinical isolates with high fluconazole MICs. 2015 Interscience Conference on Antimicrobial Agents and Chemotherapy, San Diego, CA. Poster F-763a.

570 **TABLE 1** Ligand binding affinities, azole IC_{50} values and turnover numbers for CYP51

571 proteins.

572

	K_d (nM)			
Ligand	CneoCYP51	CgruCYP51	CgatCYP51	HsapCYP51[a]
Sterols:				
Lanosterol	16300 ±2800	17300 ±900	17500 ±1900	18400 ±1500
Eburicol	13000 ±1200	11700 ±600	15800 ±1300	-
Obtusifoliol	16800 ±2100	12200 ±3000	20600 ±1000	-
Azoles:				
Clotrimazole	4 ±3	44 ±18	11 ±4	55 ±5
Fluconazole	9 ±5	52 ±15	24 ±9	30400 ±4100
Itraconazole	7 ±3	42 ±11	6 ±2	92 ±7
Ketoconazole	6 ±2	32 ±15	5 ±2	42 ±16
Voriconazole	4 ±2	14 ±9	19 ±1	2290 ±120
VT-1129	11 ±5	25 ±4	24 ±10	4530 ±300
	IC_{50} (μM)			
Azoles	CneoCYP51	CgruCYP51	CgatCYP51	HsapCYP51
Clotrimazole	-	-	-	1.9
Fluconazole	0.17	0.20	0.14	~1300 [b]
Itraconazole	0.17	0.19	0.16	70 [b]
Voriconazole	0.17	0.20	0.16	112
VT-1129	0.16	0.18	0.15	~600 [c]
	Turnover Number (min^{-1})			
Sterol	CneoCYP51	CgruCYP51	CgatCYP51	HsapCYP51[a]
Lanosterol	1.4 ±0.2	1.9 ±0.3	1.2 ±0.2	22.7 ±4.8
Eburicol	6.1 ±0.5	7.6 ±0.4	3.7 ±0.4	-
Obtusifoliol	3.5 ±0.3	3.6 ±0.3	4.5 ±0.6	-

573

574 [a] values (except for VT-1129) taken from Warrilow *et al* 2013 (24).

575 [b] values taken from Warrilow *et al* 2013 (24).

576 [c] 13% inhibition observed in the presence of 150 μM VT-1129.

577 **TABLE 2** Sterol profiles of *Cryptococcus* spp.

Sterols	Sterol composition (%)								
	C. neoformans var. neoformans			*C. neoformans var. grubii*			*C. gattii*		
	DMSO	+FLUC	+VT1129	DMSO	+FLUC	+VT1129	DMSO	+FLUC	+VT1129
Ergosta-5,7,22,24(28)-tetraenol	-	1.2 ±0.3	5.0 ±0.5	2.5 ±1.4	2.1 ±1.6	2.3 ±0.3	-	1.8 ±0.2	4.8 ±1.0
Ergosta-5,8,22-trienol	-	1.0 ±0.0	3.7 ±0.3	-	-	-	-	-	3.5 ±0.2
Ergosterol	60.6 ±2.5	42.2 ±0.7	11.5 ±3.9	43.9 ±4.3	34.1 ±3.6	18.7 ±0.6	49.3 ±9.7	52.1 ±5.5	23.2 ±2.9
Ergosta-7,22-dienol	7.4 ±0.4	-	-	9.3 ±1.1	-	-	10.8 ±6.0	-	-
Fecosterol (E8,24(28))	-	-	-	-	-	-	1.0 ±0.9	-	-
Ergosta-8-enol	-	1.6 ±0.4	-	-	-	-	-	-	3.8 ±0.5
Ergosta 5,7 dienol	-	-	-	-	-	-	3.0 ±0.6	1.8 ±0.4	-
Ergosta-7-enol	25.3 ±1.0	-	-	28.8 ±0.5	-	-	30.2 ±6.6	-	1.1 ±0.2
Eburicone	-	-	-	-	-	-	-	-	1.9 ±0.3
Lanosterol / Obtusifoliol	-	3.7 ±0.9	4.4 ±0.2	1.7 ±1.1	10.9 ±2.1	4.9 ±0.0	-	7.2 ±1.8	6.6 ±0.2
4-methyl fecosterol	-	-	-	2.5 ±0.4	-	-	-	-	-
Obtusifolione	-	35.9 ±1.8	17.1 ±1.0	-	22.1 ±1.5	24.5 ±0.6	-	20.0 ±6.0	39.4 ±2.5
Eburicol	1.5 ±0.8	12.8 ±0.7	55.8 ±5.7	6.8 ±2.0	30.0 ±2.1	49.1 ±1.1	3.1 ±2.5	13.6 ±0.7	15.4 ±1.6
4,4-dimethyl-ergosta-8,24(28)-dienol	-	-	-	4.0 ±0.8	-	-	-	-	-

578 Mean values from three replicates are shown ±SD.
579

580 **TABLE 3** Inhibition of human liver CYPs by fungal CYP51 inhibitors.
581

Inhibitor	IC_{50} (μM) [a]			
	2C9	2C19	3A4 [b]	3A4 [c]
Clotrimazole	1.4 (0.1)	0.6 (0.2)	0.03 (0.01)	0.045 (0.001)
Fluconazole	34 (10)	13 (9)	32 (5)	6 (2)
Itraconazole	80 (28)	78 (31)	0.08 (0.02)	0.13 (0.06)
Voriconazole	10 (5)	10 (4)	13 (4)	3.8 (0.2)
VT-1129	87 (21)	110 (80)	79 (23)	178 (31)

582
583 [a] Values are averages of 2 to 4 separate determinations with standard deviations in parenthesizes.

584 [b] Testosterone as substrate.

585 [c] Midazolam as substrate.

586

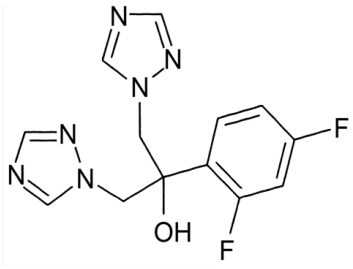

Fluconazole

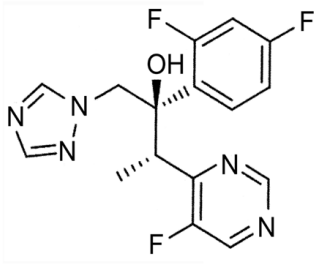

Voriconazole

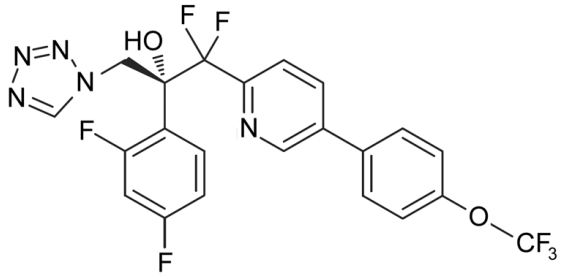

VT-1129

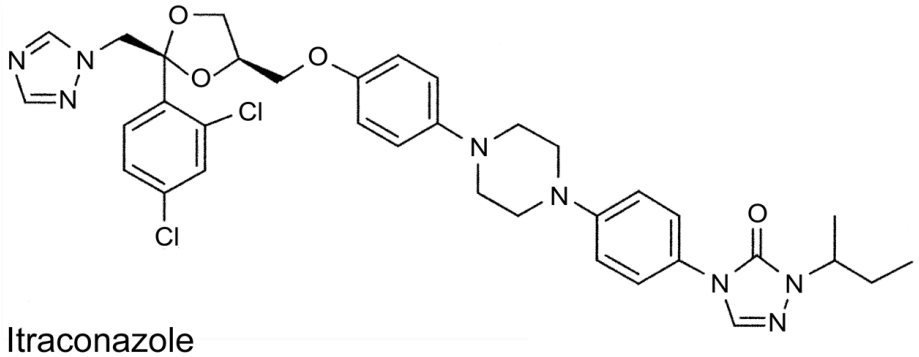

587 Itraconazole

588 **FIG 1** Chemical structures of the azole antifungals used for IC_{50} studies. The chemical
589 structures of fluconazole (molecular weight [MW], 306), voriconazole (MW, 349), VT-
590 1129 (MW, 513) and itraconazole (MW, 706) are shown.

591

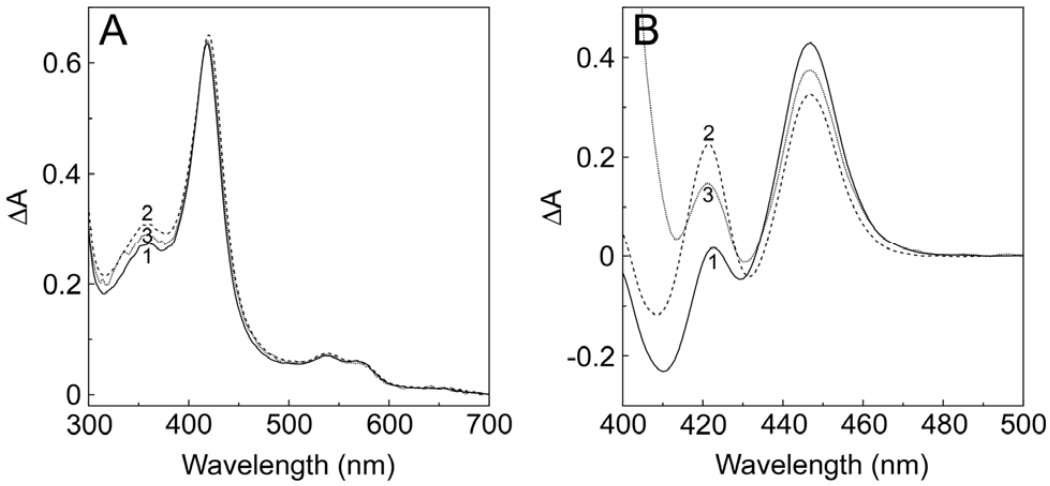

FIG 2 Absolute and reduced carbon monoxide spectra of cryptococcal CYP51 proteins. Absolute spectra in the oxidised resting state (A) and reduced carbon monoxide difference spectra (B) were determined using 5 μM solutions of purified CneoCYP51 (line 1), CgruCYP51 (line 2) and CgatCYP51 (line 3). Spectral determinations were made using quartz semi-micro cuvettes of path-length 10 mm.

604

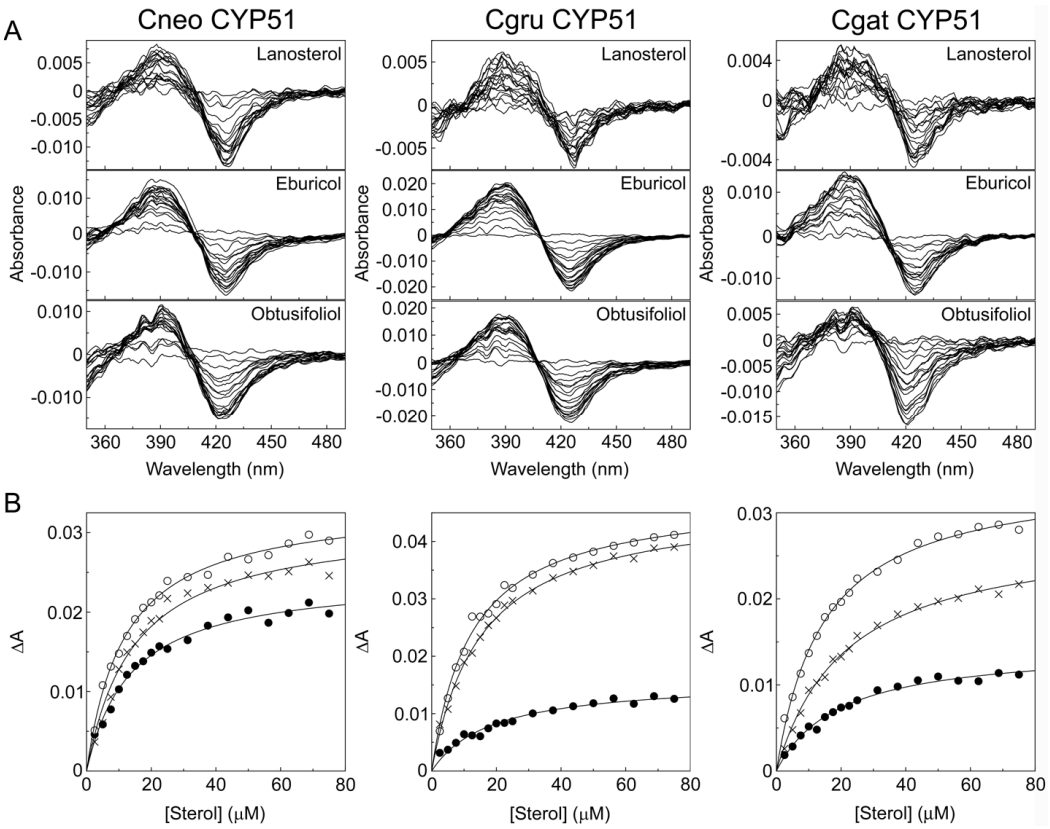

605
606

607 **FIG 3** Sterol binding properties of cryptococcal CYP51 proteins. Absorbance difference
608 spectra (A) were measured during the progressive titration of 5 μM CYP51 proteins with
609 lanosterol, eburicol and obtusifoliol. Sterol saturation curves (B) were constructed for
610 lanosterol (filled circles), eburciol (hollow circles) and obtusifoliol (crosses) with the
611 CYP51 proteins from the absorbance difference $\Delta A_{390-425}$ of the type I binding spectra
612 observed and were fitted using the Michaelis-Menten equation.

613

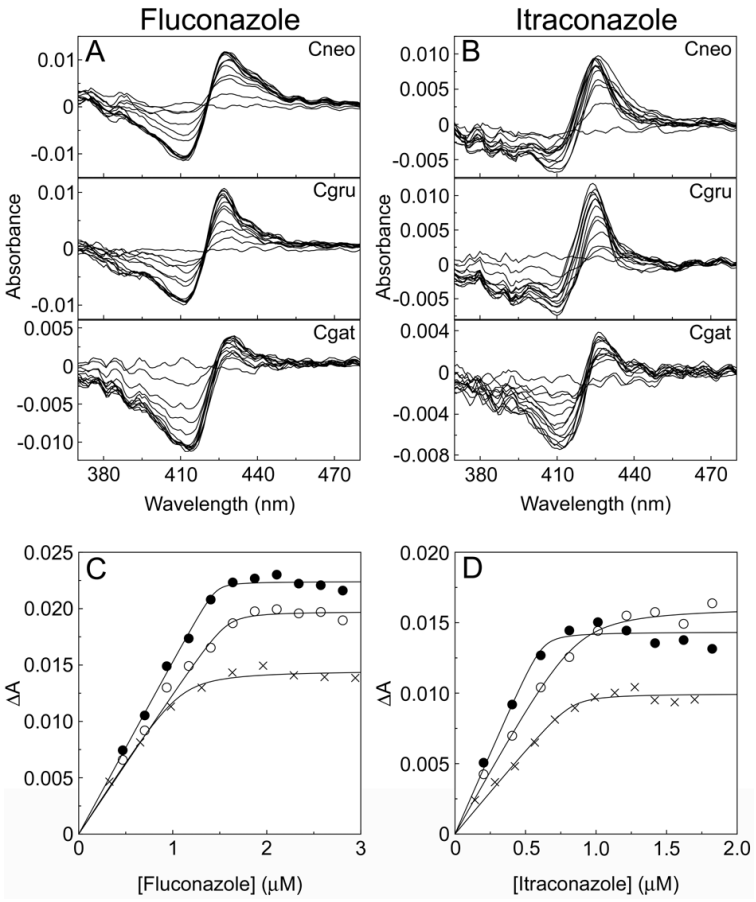

FIG 4 Azole binding properties of cryptococcal CYP51 proteins. Fluconazole and itraconazole were progressively titrated against 2 μM CneoCYP51, CgruCYP51 and CgatCYP51. The resultant type II difference spectra obtained with fluconazole (A) and itraconazole (B) are shown. Fluconazole (C) and itraconazole (D) saturation curves were constructed from the absorbance difference $\Delta A_{peak\text{-}trough}$ of the type II binding spectra observed for CneoCYP51 (solid circles), CgruCYP51 (hollow circles) and CgatCYP51 (crosses). A rearrangement of the Morrison equation was used to fit the 'tight' ligand binding observed. All experiments were performed in triplicate although only one replicate is shown.

625

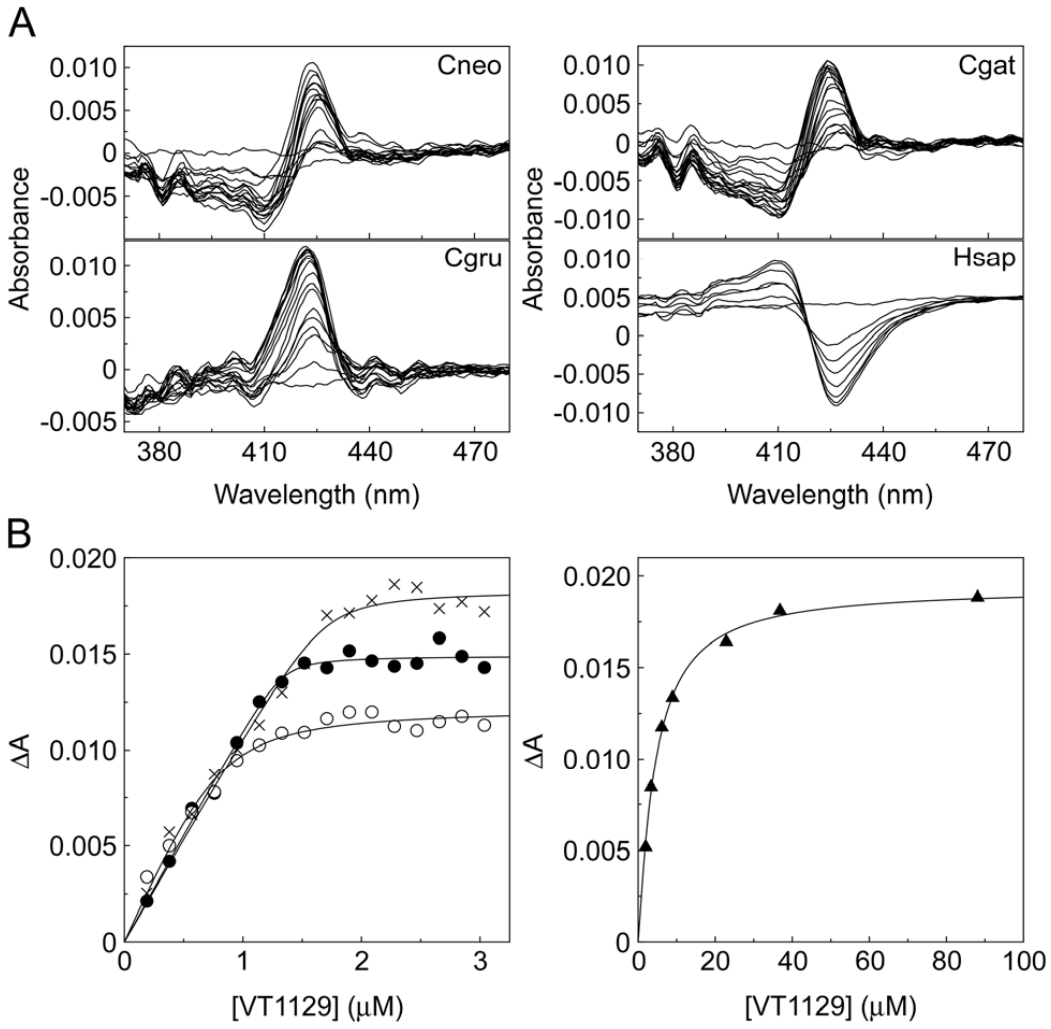

626
627

628 **FIG 5** VT-1129 binding properties of cryptococcal and human CYP51 proteins. VT-1129
629 were progressively titrated against 4 μM CneoCYP51, CgruCYP51 and CgatCYP51 and
630 5 μM human CYP51 (Hsap). The resultant type II difference spectra obtained with the
631 three cryptococcal CYP51 proteins and the red-shifted type I difference spectrum with
632 human CYP51 are shown (A). Saturation curves were constructed from the absorbance

633 difference $\Delta A_{peak\text{-}trough}$ of the type II binding spectra observed for CneoCYP51 (solid
634 circles), CgruCYP51 (hollow circles), CgatCYP51 (crosses) and human CYP51 (solid
635 triangles). A rearrangement of the Morrison equation was used to fit the 'tight' ligand
636 binding observed. All experiments were performed in triplicate although only one
637 replicate is shown.

638

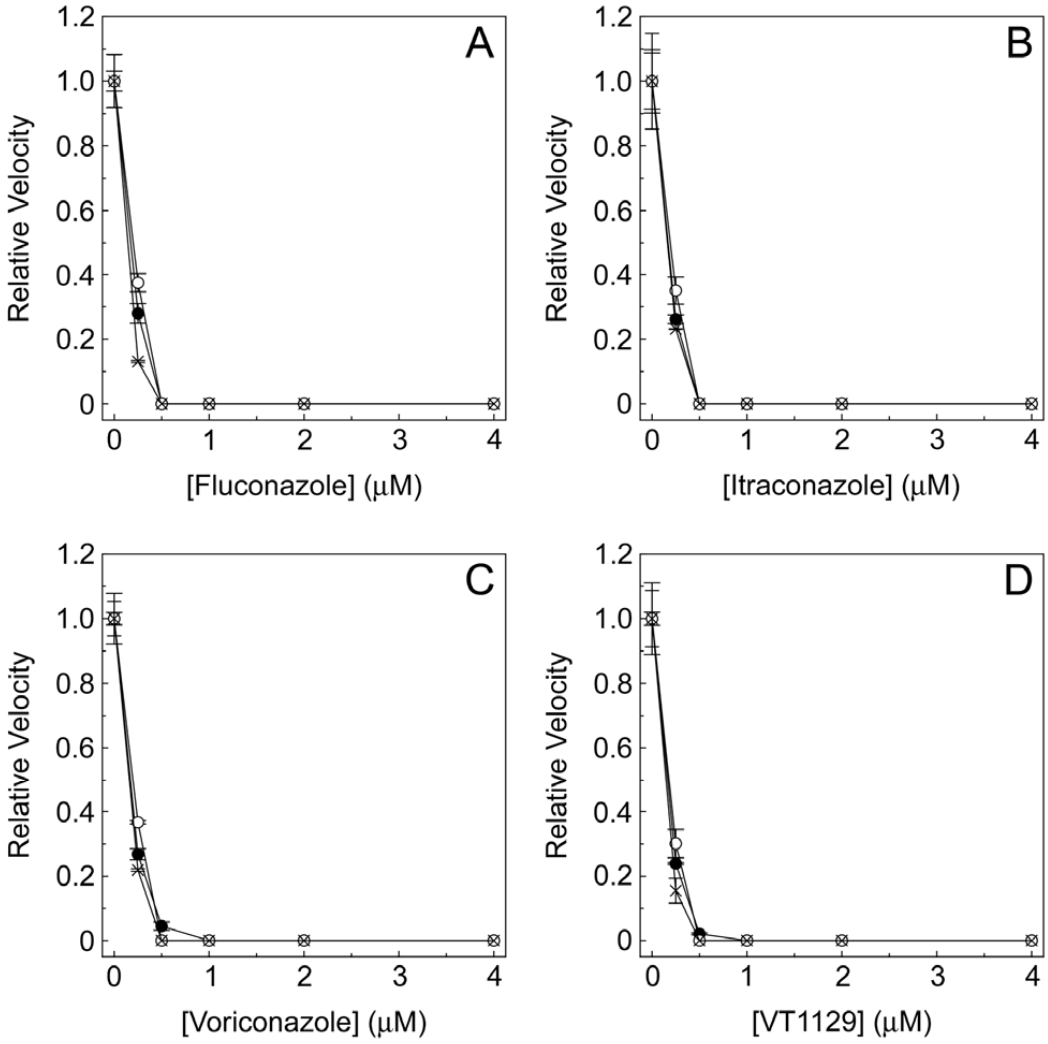

639
640

641 **FIG 6** Azole IC_{50} determinations for cryptococcal CYP51 proteins. IC_{50} values were
642 determined for fluconazole (A), itraconazole (B), voriconazole (C) and VT-1129 (D) with
643 0.5 μM CneoCYP51 (filled circles), CgruCYP51 (hollow circles) and CgatCYP51
644 (crosses) using the CYP51 reconstitution assay containing 1 μM AfCPR1 as redox
645 partner.

646

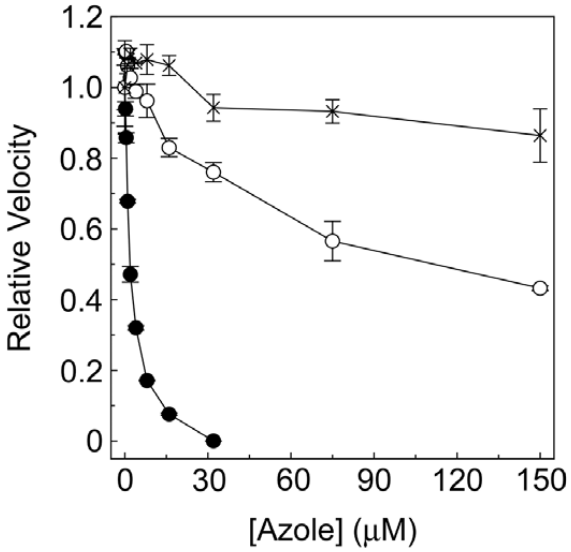

FIG 7 IC_{50} determinations with human CYP51 for clotrimazole, voriconazole and VT-1129. The CYP51 reconstitution assay contained 0.5 μM human CYP51 and 2 μM human CPR as redox partner in the presence of clotrimazole (filled circles), voriconazole (hollow circles) and VT-1129 (crosses) at concentrations ranging from 0 to 150 μM.